JOURNAL OF MATERIALS SCIENCE **40** (2005) 2335–2340

Reactive wetting of mullite $Al_2[Al_{2+2x}\ Si_{2-2x}]O_{10-x}$ single crystals by yttrium-aluminosilicate and borosilicate glasses

W. BRAUE, B. HILDMANN, H. SCHNEIDER
German Aerospace Center (DLR), Materials Research Institute, D-51147 Cologne, Germany

B. T. ELDRED, P. DARRELL OWNBY
Ceramic Engineering Department, University of Missouri-Rolla, Rolla, Missouri 65401, USA

Mullite, $Al_2[Al_{2+2x}\ Si_{2-2x}]O_{10-x}$, is introduced as a suitable reactive wetting model system for oxide ceramic compounds. Apparent contact angles on single crystal mullite substrates have been measured from sessile drop experiments involving (i) a highly reactive yttrium aluminosilicate (YAS) glass and (ii) a less reactive borosilicate (BS) glass. The apparent contact angles decrease with crystallographic orientation in the following order: (010) > (100) > (001) independent of glass composition. The surface energy, γ_{SV}, has been identified as the dominant term controlling reactive wetting with $\gamma_{SV}(010) < \gamma_{SV}(100) < \gamma_{SV}(001)$. This order of surface energy values is rationalized in terms of the high anisotropy of the crystal structure and elastic properties of mullite. The YAS glass reacts stronger with the polycrystalline 3/2 mullite substrate due to the grain boundaries acting as fast diffusion paths. In the YAS/mullite system, analytical electron microscopy shows that for the single crystal 2/1 mullite substrate, a corundum + $Y_2Si_2O_7$-rich crystalline phase assemblage results upon devitrification while in the case of the polycrystalline 3/2 mullite substrate a 2/1 mullite + $Y_2Si_2O_7$—rich crystalline assemblage is formed instead. In the less reactive borosilicate system secondary 2/1 mullite microcrystals precipitate at the S/L interface with (i) random orientations established on polycrystalline substrates and (ii) characteristic preferred orientations on the single crystal substrate. A thin Al-rich interdiffusion zone (3 μm) right at the S/L interface is revealed for both glass systems.

1. Introduction

Reactive wetting by non-crystalline grain-boundary phases is frequently observed upon densification of fine-grained oxide ceramic systems [1–4] and is important in providing the sintering mechanism and achieving control of the final microstructure [5]. Molten oxide glass on single crystal mullite is a suitable reactive wetting model system for this purpose with possibile analogies in the well-studied glass/single crystal alumina substrate system [6–10]. Besides its traditional use in refractories, mullite is a promising single phase ceramic solid solution for various structural applications because of its good thermal shock and creep resistance and excellent chemical stability (see ref. [11] for overview). Mullite, $Al_2[Al_{2+2x}\ Si_{2-2x}]O_{10-x}$, (oxygen vacancies x with $0.17 < x < 0.50$) has an oxygen-deficient orthorhombic structure covering a solid solution range between $3Al_2O_3{\cdot}2SiO_2$ (3/2 mullite, $x = 0.25$) and $2Al_2O_3{\cdot}SiO_2$ (2/1 mullite, $x = 0.40$) [11]. In a previous study [12] the wetting behavior of polycrystalline 3/2 mullite has been investigated involving two different glass batches: (i) a highly reactive yttrium-aluminosilicate glass (YAS) and (ii) a less reactive borosilicate glass (BS). It was found that both glasses wet polycrystalline mullite but the YAS glass wet significantly better than the borosilicate system showing more penetration of the substrate along the grain boundary network.

In the present study this approach is expanded towards oriented (100), (010) and (001) slices from Czochralski-grown mullite single crystals in order to address possible orientation effects during the reactive wetting of mullite. An interpretation of the orientation dependance of the apparent contact angles measured during the sessile drop experiments is offered in light of the structural anisotropy of the mullite crystal structure and elastic properties. The nanoscale microstructure of the solid/liquid interface is investigated by means of analytical electron microscopy. Devitrification of the more reactive YAS glass upon cooling is addressed in terms of phase relationships in the ternary Y_2O_3-Al_2O_3-SiO_2.

2. Experimental procedure

Mullite single crystals have been grown by the Czochralski techniques (courtesy F. Wallrafen, University of Bonn, Germany) following the concept of Guse and Mateika, 1974 [13]. With 76.7 wt% Al_2O_3 and 23.3 wt% SiO_2, the bulk composition of the single crystals is close to 2/1 mullite ($x = 0.385$). The residual deviation from precise orientation for (100), (010) and (001) slices was less than 0.2° as verified by high-resolution X-ray diffraction. The slices were polished with 3 μm diamond followed by 0.1 μm alumina (estimated residual roughness ≤ 1 μm).

The polycrystalline 3/2 mullite substrate material was produced by sintering high-purity, fine-grained commerical powders. Processing of this material is discussed elsewhere [5] in full detail. Two glass batches were employed in this study: (i) a yttrium-aluminosilicate glass (YAS-6, for characterization see ref. [14]) having a bulk composition of 42 wt% Y_2O_3, 25 wt% Al_2O_3, and 33 wt% SiO_2 and (ii) a commercial borosilicate glass (CORNING Inc.) with approx. 74.5 wt% SiO_2, 19 wt% B_2O_3, 4.5 wt% Na_2O, 2 wt% Al_2O_3.

The sessile drop experiments were carried out in air utilizing a high-purity alumina tube furnace heated by a molybdenum wound element. The actual temperature of the sample was monitored to ±2°C with an optical pyrometer sighted on the glass drop. For each experiment, the furnace was slowly heated to 300°C to prevent damage to the element, then ramped at 2°C/min from 300 to 1330°C, and finally ramped at 1°C/min from 1330 to 1600°C. After reaching 1600°C, the furnace was cooled at 5°C/min to 600°C, then the power was turned off and the furnace was allowed to air cool to room temperature. During softening, each drop was filmed continuously with a digital video camera, and still frames at 720 × 480 dpi were captured every two minutes. The mass of the drops was typically in the 0.01–0.02 g range. When the contact angle neared equilibrium, the drops were filmed every fifteen minutes. Adobe Photoshop 5.5 was used to measure the apparent contact angle to ±2°, and an average of four measurements was used for each data point. Following WARRENs terminology [15] the term "apparent contact angle" is employed in order to account for non-planar S/L interfaces during reactive wetting. Cross-section specimens for SEM analysis (LEO Gemini 982) were prepared from the solidified drops by sectioning normal to the S/L interface with a thin diamond wafering blade followed by polishing to 0.03 μm with alumina.

3. Results and discussion

3.1. Apparent contact angle measurements

The measured apparent contact angles of the borosilicate glass as a function of temperature are shown in Fig. 1. All samples on single crystal substrates underwent a gradual softening between about 1300 and 1450°C, achieving a steady state above 1450°C.

As compared to the (010) and (100) experiments, the (001) sample softened slightly earlier and also reached steady-state conditions earlier, but the shape of the curve is similar to (010) and (100). At 1600°C the (001) sample had the lowest apparent contact angle, 28°, of the borosilicate samples. Sample (100) had an apparent contact angle of 45°, and (010) had the highest apparent contact angle of 64°. The polycrystalline sample followed a simple rule of mixtures, with an equilibrium angle of 43°.

Fig. 2 shows the apparent contact angles of the YAS glass as a function of temperature. These samples exhibited an almost crystal-like melting, transforming from the angular, as-received pieces to low-contact-angle, molten drops over the temperature range 1400–1425°C. Above 1425°C, the (001) sample quickly reached an a constant contact angle of 6°, but

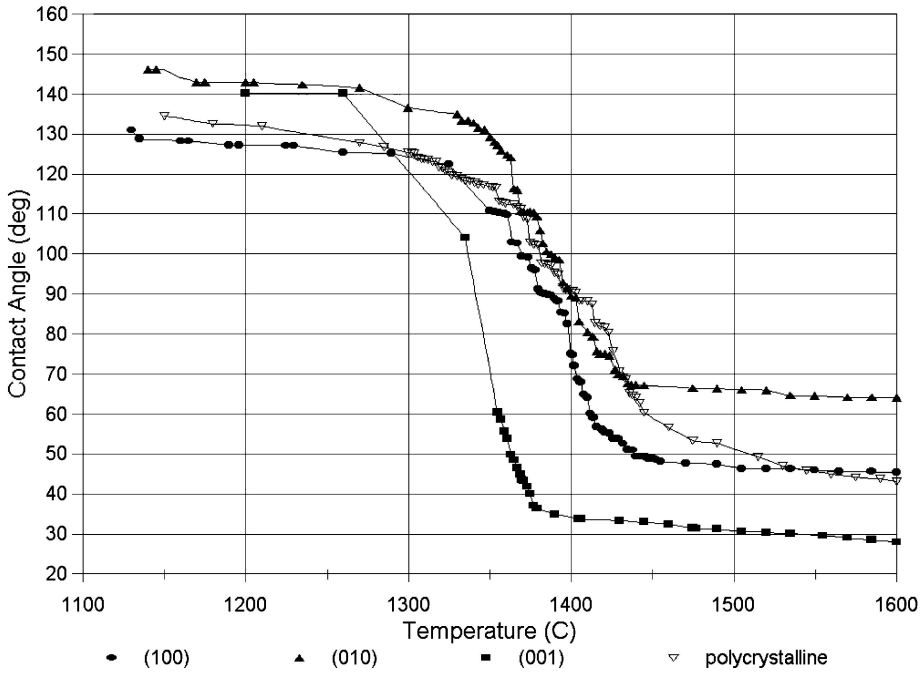

Figure 1 Apparent contact angles of borosilicate glass on (100), (010), (001) and polycrystalline mullite.

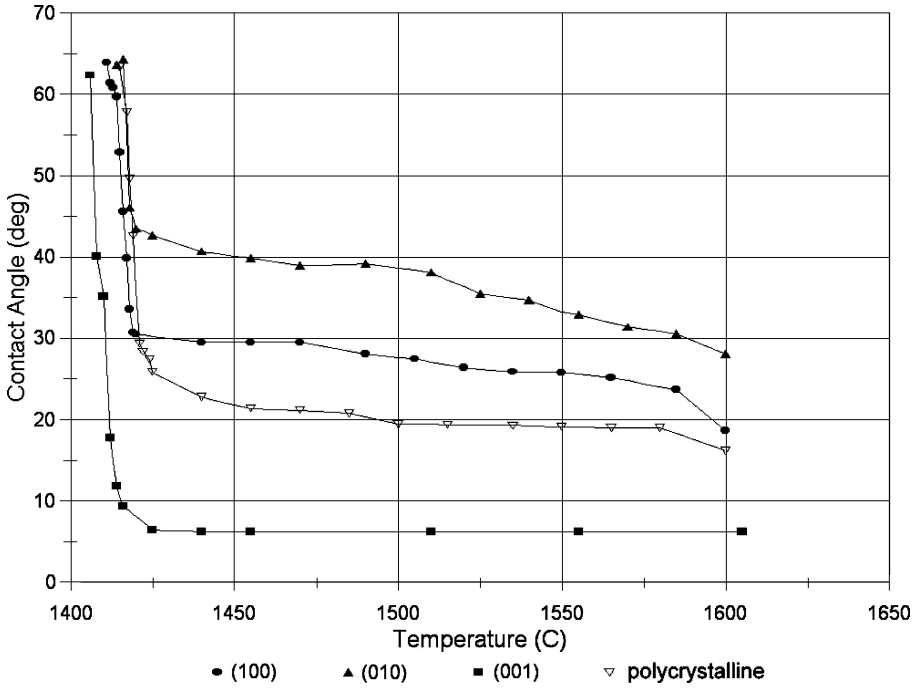

Figure 2 Apparent contact angles of YAS glass on (100), (010), (001) and polycrystalline mullite.

the other samples continued to decrease in contact angle throughout the experiment. At 1600°C the (100) and (010) samples reached contact angles of 19° and 28°, respectively, with approximately the same slope of $-3 \times 10^{-2}\,^{\circ}C^{-1}$, and the polycrystalline sample showed rule of mixtures behavior with a final contact angle of 16°, again in- between the (100) and (001) curves.

This wetting phenomena cannot be adequately explained by classic wetting theory such as the Young-Dupré equation. Since the composition of the liquid in the interfacial region is constantly changing due to dissolution of the substrate, local chemical reactions, and precipitation of refractory devitrification products (see Section 3.2), the local surface energies can be very different from the surface energies of the bulk, as-received glass. Reactive wetting of ceramics by metals has been extensively investigated [16–20] and it is generally concluded that extra terms must be added to the Young-Dupré equation to account for the additional energy of reaction. Most commonly, the reaction will decrease the solid-liquid interfacial energy, leading to a decrease in the contact angle. However, reactions that increase γ_{SL} and thus the apparent contact angle have also been detected. The same principles may apply in this study: the reaction between the two glasses and the mullite substrates may decrease γ_{SL} and cause a drop of apparent contact angle.

Significantly for both glasses investigated, the apparent contact angles follow the same sequence: the (001) substrate had the lowest angle, followed by the polycrystalline, (100), and (010) consecutively. Obviously this wetting anisotropy is rather insensitive to composition and reactivity of the glass system but is controlled by the anisotropy of mullite surface energies.

Although the dynamic dissolution rates are different for (100), (010) and (001) orientations, γ_{LV} is expected to be fairly independent of substrate orientation. While γ_{SL} is most likely to be reduced during interfacial reactions, its orientation dependence remains unclear at this point. The solid-vapor interfacial energy, γ_{SV} is proposed to represent the dominant orientation-dependent term in the wetting behavior of mullite. Since for a wetting system ($\Theta < 90^{\circ}$), increasing γ_{SV} while keeping other factors constant results in a decrease of apparent contact angle, the following orientation dependence of γ_{SV}, namely γ_{SV} (010) $< \gamma_{SV}$ (100) $< \gamma_{SV}$ (001), may be anticipated from Figs 1 and 2.

The anisotropy of mullite surface energies may be rationalized in terms of the pronounced anisotropy of the crystal structure and elastic properties of mullite. Stiff tetrahedra chains extend parallel to the *c*-axis and are stabilized against tilting by chains of edge-sharing AlO_6 octahedra thus giving rise to a high stiffness coefficient c_{33} (352 GPa) referring to tensile stiffness parallel to the *c*-axis. Perpendicular to the *c*-axis, the mullite structure does not exhibit continuous chains. Consequently, the corresponding stiffness coefficients are significantly lower ($c_{11} = 291$ GPa, $c_{22} = 233$ GPa, for overview see [21]) indicating that the anisotropy of the surface energy γ_{SV} does indeed follow γ_{SV} (010) $< \gamma_{SV}(100) < \gamma_{SV}(001)$.

3.2. Microstructural constraints of reactive wetting of mullite

The S/L interface reveals a flat *w*-shaped morphology (Fig. 3). A comparison with calculated shapes of the liquid phase during reactive wetting [22, 23] emphasizes that thermodynamic equilibrium has not yet been established during the duration of the sessile drop experiments. Fig. 3 also emphasizes that during continuous evaluation of wetting the apparent contact angle Θ_{app} (which must not be confused with Θ_{Young}) is the only one that is measurable.

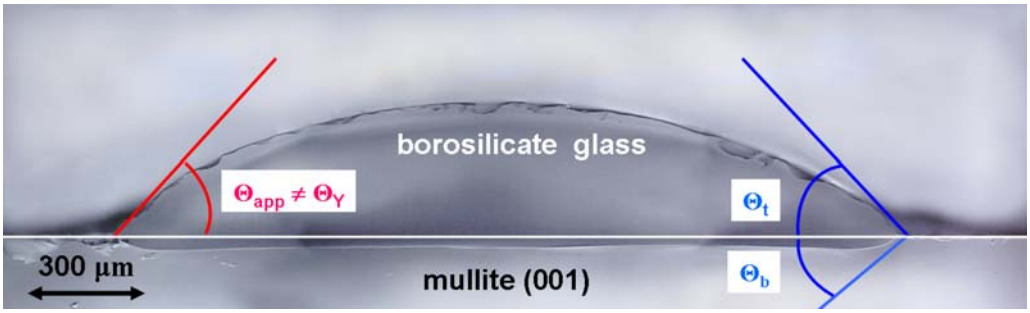

Figure 3 Optical micrograph obtained from the polished cross-section of the less reactive borosilicate glass on the mullite (001) substrate revealing the flat, "*w*-shaped" morphology of the liquid/solid interface established after reactive wetting. White line refers to mullite substrate surface prior to the sessile drop experiment.

Due to dissolution of the single crystal mullite substrate a thin (3 μm) interdiffusion zone consisting of Al-enriched mullite could be confirmed via analytical electron microscopy for both the borosilicate and YAS glasses. For the borosilicate system the interdiffusion zone is followed by oriented growth of secondary 2/1 mullite microcrystals into the residual glass. Note that for the polycrystalline substrate the growth of 2/1 mullite needles is random while those above the single crystal substrates are all oriented in the [001] direction (Fig. 4).

In contrast to the borosilicate glass, the yttria-aluminosilicate glass (YAS-6) reacted strongly with both single crystal and polycrystalline mullite substrates. Fig. 5 shows low magnification images of cross-sections of the (100) and polycrystalline samples.

The difference in the appearance of the single crystal and polycrystalline samples is directly attributable to the presence of grain boundaries. As reported in a previous paper [12] and verified in this work, YAS glass wets mullite very well, with contact angles down to 6° for the (001) facet at 1600°C (Fig. 2). Such a low contact angle makes it very likely that the glass will penetrate predominantly along the grain boundaries of the polycrystalline sample. Thus, during the experiment each mullite grain in the penetration zone is attacked on many sides by an intergranular glass film. The single crystal substrate, in contrast, offers much less surface area and a consequently lower dissolution rate. As seen in Fig. 5 (bottom), the penetration zone extends deeply into the polycrystalline substrate on a mm-scale.

Moreover, for the single crystal substrates, a strongly serrated S/L interface is observed in the direction of fast growth in corundum, that is parallel to the basal planes, is actually inclined relative to the S/L interface (Figs 5 top and 6 left). The S/L interface remains smooth in case

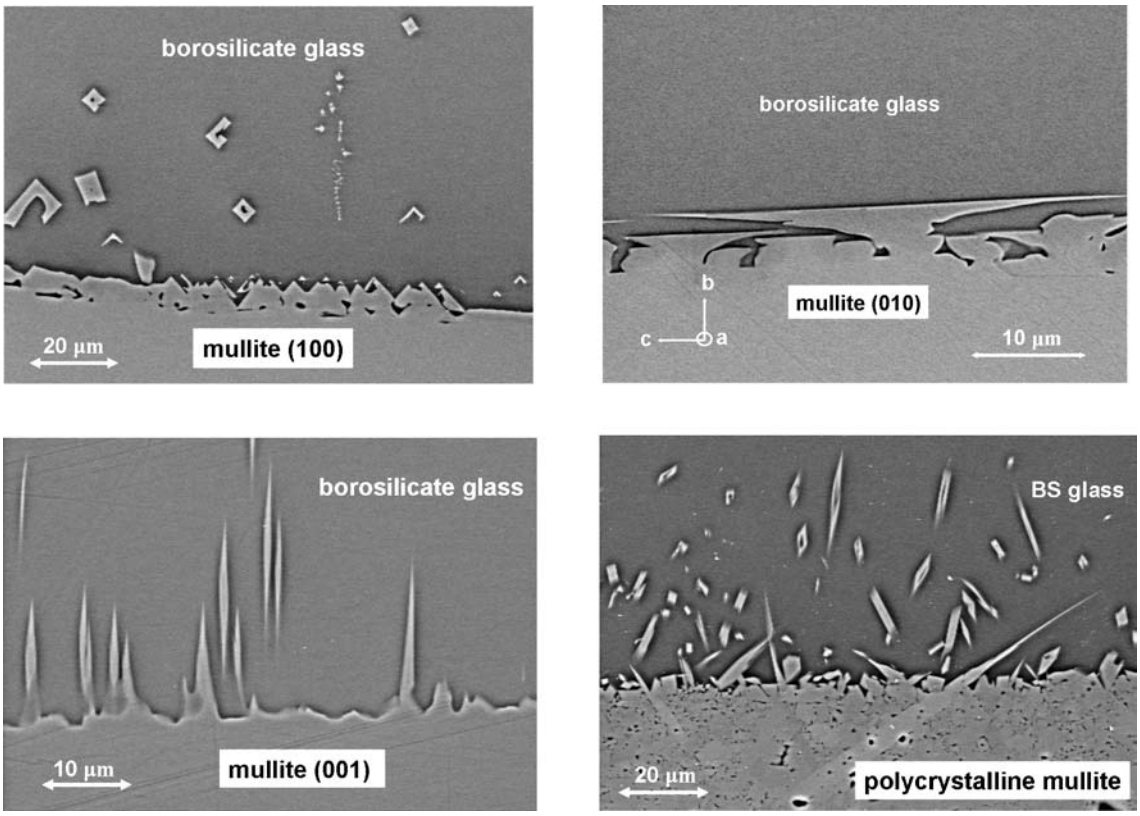

Figure 4 Instability of the solid/liquid interface due to partial dissolution of the mullite substrate (close to 2/1 compositon, $x < 0.40$) in borosilicate glass followed by (i) oriented growth of Al-enriched mullite needle-like oriented microcrystals (2/1 compositon, $x = 0.40$) for single crystal mullite substrates, and (ii) random growth for the polycrystalline substrate upon cooling.

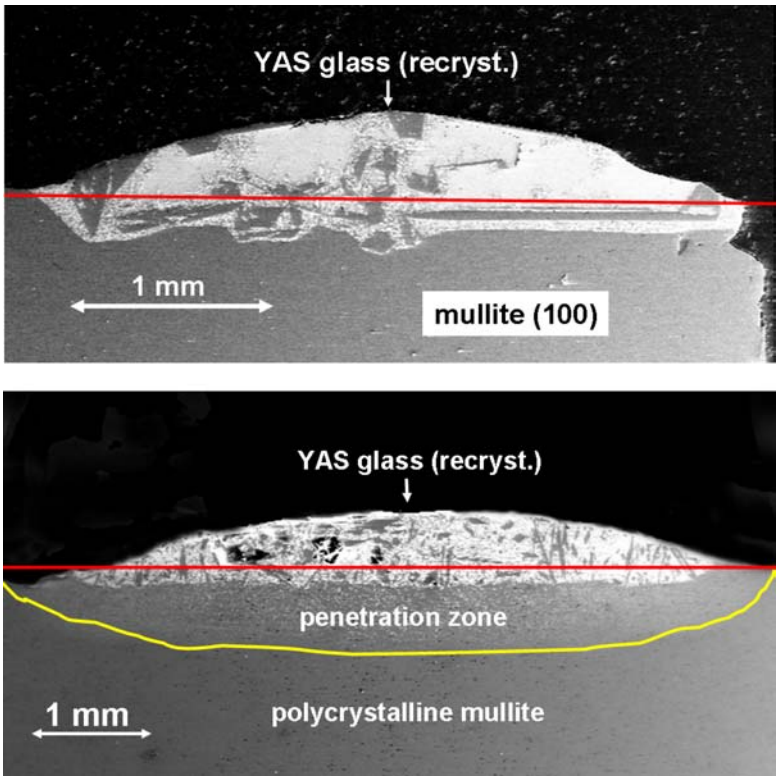

Figure 5 SE images obtained from polished cross-sections of YAS glass on single crystal substrate (top) and polycrystalline substrate (bottom). A reference line referring to the planar mullite substrates prior to the sessile drop experiment is included for comparison. Note the extensive penetration zone of the glass into the polycrystalline substrate that is enhanced by the grain boundary network.

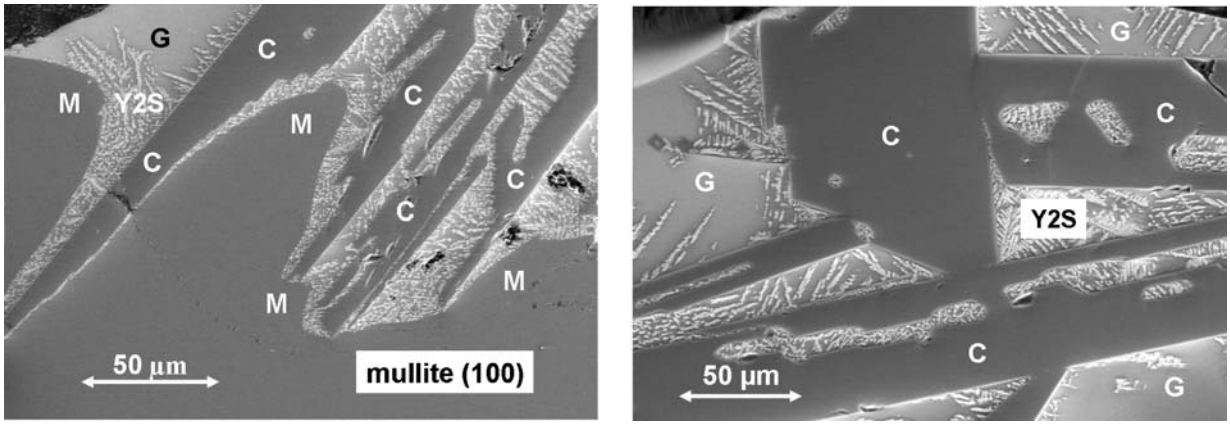

Figure 6 Higher magnification (SE images) of YAS glass on single crystal 2/1 mullite (100) substrate. Note strongly serrated S/L interface due to mullite substrate (M) dissolution followed by fast corundum (C) growth (left). Devitrification upon cooling (right) results in formation of large corundum plates (C), large pockets of a residual glass (G), imbedded with dendritic $Y_2Si_2O_7$ (Y2S) grains and very few mullite crystals.

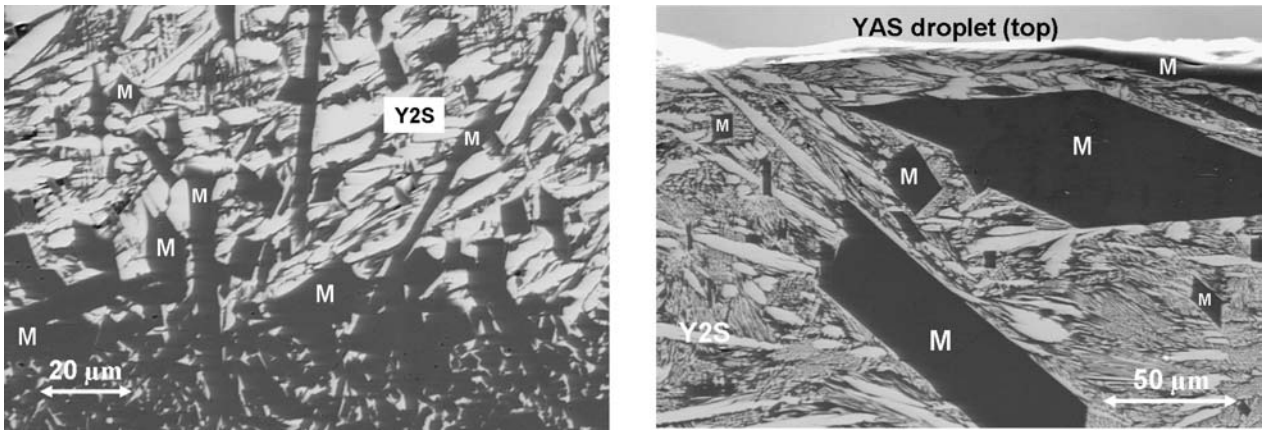

Figure 7 SE-images from the microstructure of YAS on the polycrystalline 3/2 mullite substrate: predominant growth of 2/1 mullite crystals and $Y_2Si_2O_7$ at the S/L interface (left), and top of the YAS glass droplet (right)

of corundum plates growing parallel to the interface (Fig. 5 top, right hand side).

For the highly reactive YAS system the combined effects of mullite dissolution and devitrification upon cooling cause the initial YAS-6 bulk compositon to shift its original position close to the ternary peritectic point in the Y_2O_3-Al_2O_3-SiO_2 system (see [23] for overview) toward the 2/1 mullite composition into the Al_2O_3 primary crystallization field. In the case of the dissolution of the 3/2 polycrystalline mullite substrate the composition is shifted towards the mullite primary crystallization field of the ternary phase diagram because of the additional SiO_2 in the grain boundaries. This different microstructure is addressed in Fig. 7 emphasizing the effects of different Al/Si ratios in the substrate compositions (2/1 versus 3/2 mullite) imposed on the crystallization paths during cooling.

4. Conclusions

The yttrium-aluminosilicate, YAS, glass reacts strongly with both single crystal and polycrystalline mullite to produce characteristic morphologies of the S/L interface and a complex phase assemblage upon cooling involving corundum and/or mullite, $Y_2Si_2O_7$, and a residual non-devitrified phase, depending on the type of mullite substrate. The relevant crystallization paths upon devitrification can be derived from phase relationships in the ternary Y_2O_3-Al_2O_3-SiO_2. The less reactive borosilicate glass simply dissolves a portion of the substrate and precipitates secondary 2/1 mullite microcrystals near the interface on cooling.

The apparent contact angles of both glasses increase with crystallographic orientation of the substrate in the following order: (001) < polycrystalline < (100) < (010). This is in agreement with previous studies which show the (001) plane to have the highest energy of the three principal planes in mullite. The apparent contact angles of the YAS glass are significantly lower than those of the borosilicate glass due to the reactive wetting.

This research has demonstrated the potential of mullite as a suitable model system for reactive wetting studies. Work is currently underway to direct the issue of wetting of external mullite surfaces towards internal interfaces of fully densified sintered mullite ceramics in order to address the effects of grain boundary orientations and local chemistry at grain boundaries.

References

1. D. R. CLARKE and M. L. GEE, in "Materials Interfaces, Atomic-Level Structure and Properties", 1st ed. edited by D. Wolf and S. Yip (Chapman & Hall, 1992) p. 255.
2. H. J. KLEEBE, G. HILZ and G. ZIEGLER, *J. Am. Ceram. Soc.* **79** (1996) 2592.
3. F. KARA, S. TURAN, J. A. LITTLE and K. M. KNOWLES, *ibid.* **83** (2000) 369.
4. W. BRAUE, R. PLEGER, G. PAUL, H. SCHNEIDER and J. DECKERS, *J. Eur. Ceram. Soc.* **16** (1996) 85.
5. T. S. HUANG, M. N. RAHAMAN, T. MAH and T. A. PARTHASARATHAY, *J. Am. Ceram. Soc.* **83**(1) (2000) 204.
6. Y. K. SIMPSON and C. B. CARTER, *ibid.* **73** (1990) 2391.
7. P. DARRELL OWNBY, K. W. K. LI and D. A. WEIRAUCH, *ibid.* **74** (1991) 1275.
8. D. KIM, S. M. WIEDERHORN, B. J. HOCKEY, C. A. HANDWERKER and J. E. BLENDELL, *ibid.* **77** (1994) 444.
9. J. K. PARK, D. Y. KIM, H. Y. LEE, J. BLENDELL and C. HANDWERKER, *ibid.* **86** (2003) 1014.
10. G. LEVI and W. D. KAPLAN, *Acta Mater.* **51** (2003) 2793.
11. H. SCHNEIDER, K. OKADA and J. PASK, "Mullite and Mullite Ceramics", (J. Wiley, New York, 1994).
12. T. S. HUANG, M. N. RAHAMAN, B. T. ELDRED and P. D. OWNBY, *J. Mater. Res.* **16**(11) (2001) 3223.
13. W. GUSE and D. MATEIKA, *J. Cryst. Growth* **22** (1974) 237.
14. M. J. HYATT and D. E. DAY, *J. Am. Ceram. Soc.* **70** (1987) C 283.
15. J. A. WARREN, W. J. BOETTINGER and A. R. ROOSEN, *Acta Mater.* **46** (1998) 3247.
16. J. CHEN, M. Y. GU and F. S. PAN, *J. Mater. Res.* **17**(4) (2002) 911.
17. B. DREVET, K. LANDRY, P. VIKNER and N. EUSTATHOPOULOS, *Scripta Mater.* **35**(11) (1996) 1265.
18. X. B. ZHOU and J. T. M. DEHOSSON, *Acta Mater.* **44**(2) (1996) 421.
19. D. A. WEIRAUCH, W. M. BALABA and A. J. PERROTTA, *J. Mater. Res.* **10**(3) (1995) 640.
20. S. KALOGEROPOULOU, L. BAUD and N. EUSTATHOPOULOS, *Acta Mater.* **43**(3) (1995) 907.
21. B. HILDMANN, H. LEDBETTER, S. KIM and H. SCHNEIDER, *J. Am. Ceram. Soc.* **84** (2001) 2409.
22. N. EUSTATHOPOULOS, M. G. NICHOLAS and B. DREVET, "Wettability at High Temperatures", (Pergamon Press, 1999).
23. O. FABRICHNAYA, H. J. SEIFERT, R. WEILAND, T. LUDWIG, F. ALDINGER and A. NAVROTSKY, *Z. Metallkd.* **92** (2001) 1083.

Received 31 March
and accepted 18 July 2004